New apparatus for thermomechanical analogue modeling

Article *in* Memoir of the Geological Society of America · January 2001

DOI: 10.1130/0-8137-1193-2.245

CITATIONS
5

READS
52

4 authors, including:

Djordje Grujic
Dalhousie University
101 PUBLICATIONS **5,531** CITATIONS
SEE PROFILE

Robert Hofmann
Eth Zürich Switzerland
1 PUBLICATION **5** CITATIONS
SEE PROFILE

Jan H. Behrmann
GEOMAR Helmholtz Centre for Ocean Research Kiel
475 PUBLICATIONS **4,105** CITATIONS
SEE PROFILE

Geological Society of America
Memoir 193
2001

New apparatus for thermomechanical analogue modeling

Elmar M. Wosnitza, Djordje Grujic
Geologisches Institut der Universität Freiburg, Albertstraße 23 B, D-79104 Freiburg, Germany
Robert Hofmann
Gundrebenstrasse 3, CH-8932 Mettmenstetten, Switzerland
Jan H. Behrmann
Geologisches Institut der Universität Freiburg, Albertstraße 23 B, D-79104 Freiburg, Germany

ABSTRACT

A new apparatus designed for thermomechanical analogue modeling to investigate tectonic crustal-scale processes, in particular the role of rheology in the distribution and propagation of deformation, is presented. By inducing a vertical thermal gradient through suitable analogue materials and controlling heat flow into the bottom and out of the top of the model, a precise viscosity gradient can be obtained. For the temperature range employed, paraffin wax shows a viscosity range of more than 11 orders of magnitude. A maximum of ~60% shortening or 200% extension is possible in the horizontal direction. The machine can determine the applied force, the horizontal shortening, and the model height at two locations. The bulk rheology is estimated from the calculated stress and the imposed constant strain rate, which can be varied between 10^{-6} and 4×10^{-5} s^{-1}. The two-dimensional temperature distribution of the glass confining side walls is measured with a thermal infrared camera and is proportional to the temperature distribution within the model. Deformation of the isotherms can thus be monitored during the experiment. By scaling down linear dimensions by a factor of 10^6, time by 10^{10}, viscosity by 10^{16}, and temperature by 10, we obtain a consistent set of scaling factors. This allows geometrical, kinematic, dynamic, and rheological similarity with lithospheric processes to be attained.

INTRODUCTION

To simulate the rheological stratification of the Earth's crust in physical models, it is necessary to take into account the variations in mechanical properties induced by variations in temperature. Until now this has been done experimentally by using different materials, such as sand and silicone putty, to model brittle and ductile behavior, respectively (e.g., Davy and Cobbold, 1991). Major progress has been made in this way in understanding crustal and lithospheric processes (e.g., Chemenda et al., 1995). However, the major drawback with such models is that any material point within the model crust retains its physical properties throughout the experiment, regardless of its changing position within the model. Thermal readjustment is not taken into account, and proper scaling with respect to gravity is therefore not achieved.

Analogue experiments to model crustal processes using temperature dependent material properties have been made before. However, none of them has fully exploited the possibilities. Oldenburg and Brune (1972, 1975) focused on freezing the material, but did not use the temperature dependency of viscosity. Shemenda and Grocholsky (1994) and Brune and Ellis (1997) used a temperature-sensitive viscosity, but did not map the temperature distribution in the material. Nataf and Richter (1982) examined convection in fluids with temperature-dependent viscosity and mapped isolines of the thermal gradient, applying their results to the evolution of planets.

The advantage of building models with a temperature-sensitive viscosity is that the mechanical consequences of thermal readjustment during the experiment can be reproduced. Our approach was to apply this concept to crustal rheological stratification and to map the temperature distribution. This represents

Wosnitza, E.M., et al., 2001, New apparatus for thermomechanical analogue modeling, *in* Koyi, H.A., and Mancktelow, N.S., eds., Tectonic Modeling: A Volume in Honor of Hans Ramberg: Boulder, Colorado, Geological Society of America Memoir 193, p. 245–251.

a major improvement in analogue models of plate tectonic processes. It is particularly significant for experiments investigating lithospheric stretching and the stability of mountain belts. For example, in subduction zones the material balance is strongly controlled by the rheology of the subducted sediments (e.g., Mancktelow, 1995). This concept has also been applied to exhumation in collision zones (e.g., Grujic et al., 1996).

To investigate convergence processes, in particular the role of rheology in the distribution and propagation of deformation, a deformation rig was designed especially for thermomechanical modeling. Analogue materials with a temperature-sensitive viscosity are used to simulate the change of mechanical properties with depth. Correlating the thermal field with the displacement field and the material distribution allows the rheological structure of the model to be deduced.

APPARATUS

Overview

The usable model dimensions of the rig are 35 cm width, 25 cm height, and 50 cm length. Models can be either shortened by 60% or extended by 200% under plane strain (Fig. 1). The upper surface of the model is unconfined. The force is applied to the model through two Teflon-coated wooden pistons. This choice of material offers the most economical combination of strength and thermal insulation. Due to its high thermal conductivity, a metal piston would lead to significant boundary effects. A slit below the pistons allows material to flow behind the pistons, maintaining isostatic equilibrium. The pistons move symmetrically, but they can be independently activated. The side walls are made of glass with a thermal diffusivity similar to that of the analogue materials used in our experiments.

To apply a thermal gradient, the temperature has to be controlled at two levels within the model. The model is therefore both heated from below and cooled from above by two independent thermostats. The apparatus and thermostats are controlled, and data are quasicontinuously acquired with a microcomputer and a 12-bit analogue to digital converter card, using software developed under LabVIEW® Version 5 (Jamal and Pichlik, 1997).

Controlled and measured parameters

The graphical user software interface displays all measured properties, both numerically and graphically. Three parameters, i.e., the desired strain rate and the upper and lower temperatures, are controlled during the experiments. They can be set at the start of an experiment, and maintained constant during the run.

Strain rate and velocity. Most motors suitable for deformation experiments generate constant velocities only for a given time interval. Preliminary calibration experiments showed that the motor adequately maintained the desired velocities, and that correction for this error is unnecessary.

During the test phase a constant strain rate $\dot{\varepsilon}$ was maintained to remove one of the variables controlling viscosity. In these experiments, methods of motor control based on the variation of the model length l with time t can be obtained by integration of

$$\dot{\varepsilon} = \frac{\mathrm{d}l(t)/l(t)}{\mathrm{d}t}, \tag{1}$$

which leads to

$$l(t) = l(0)e^{\dot{\varepsilon}t}. \tag{2}$$

Because the velocity v was constant over the time interval Δt, this results in a deviation of the actual strain rate $\dot{\varepsilon}_a$ from the required strain rate $\dot{\varepsilon}$. The velocity v was recalculated at the beginning of each Δt using l_0, the length of the model at that time. The actual strain rate is calculated as

$$\dot{\varepsilon}_a(t) = \frac{v}{l_0 + vt}. \tag{3}$$

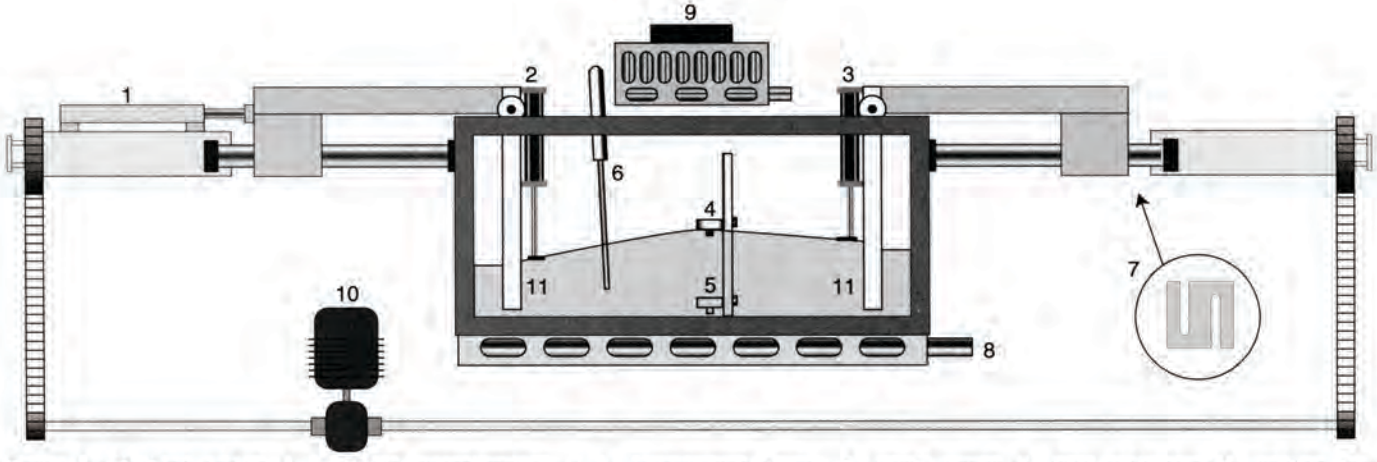

Figure 1. Machine design. 1–3—linear potentiometers, 4–6—temperature probes, 7—strain gauge, 8—heat exchanger, 9—cooling fan, 10—motor, 11—pistons.

To minimize the error, we use the secant of $l(t)$ to determine the desired velocity. From the required lengths at the beginning and the end of the time step, we obtain

$$v(t) = \frac{l(0)e^{\dot{\varepsilon}(t+\Delta t)} - l(0)e^{\dot{\varepsilon}t}}{\Delta t} = \frac{l(t)}{\Delta t}\left(e^{\dot{\varepsilon}\Delta t} - 1\right). \quad (4)$$

The mean actual strain rate $\bar{\dot{\varepsilon}}_a$ during Δt, obtained from integration of equation 3 over Δt, is

$$\bar{\dot{\varepsilon}}_a = \frac{e^{\dot{\varepsilon}\Delta t} - 1}{(\Delta t)^2} \int_0^{\Delta t} \frac{1}{1 + (e^{\dot{\varepsilon}\Delta t} - 1)\dfrac{t}{\Delta t}}\, dt$$

$$= \frac{1}{\Delta t} \ln(e^{\dot{\varepsilon}\Delta t}) = \dot{\varepsilon}. \quad (5)$$

Thus, the mean actual strain rate corresponds to the required strain rate, independent of the duration of the time step.

The motor and the gears allow the strain rate to be set between 2×10^{-6} s^{-1} and 2×10^{-4} s^{-1}. Strain rates can be maintained constant to within 5%. With a linear potentiometer the position of one of the pistons is monitored with an accuracy of <1 μm, thus allowing actual strain rates to be determined using the internal clock of the controlling computer.

Temperatures. The temperature field is controlled at two levels within the model. Two temperature probes at the base and at the top of the model are connected to a heating and a cooling thermostat, respectively. The model can be heated to temperatures up to 150 °C from below using a thermostat and silicone oil for the heat transfer. A cooling fan above the model connected to a second thermostat allows the model surface to be maintained between 20 and 80 °C. The thermostats are able to maintain the temperatures to within 0.1 °C in the steady state. To achieve a stable temperature gradient the model must be preheated for at least 10 hr.

Once they are set by the computer, the thermostats automatically maintain the temperature at their respective probes by using fuzzy-logic software. The computer receives, displays, and stores the temperature time series at the desired sampling rate.

The entire machine is insulated by a box of styrofoam to keep overall temperature conditions constant during experiments. A horizontal layer of styrofoam around the model separates the upper part from the lower part of the box, insulating the higher temperatures at the bottom of the model from the lower temperatures at the top. In addition to the temperature probes mentioned above, a third probe is embedded in the model. All the temperature probes are calibrated to ~0.05 °C.

Stress. To determine the bulk rheology of the model, the force applied to the model during the experiment is monitored by a strain gauge with a tolerance of 0.1%. In addition, the material height, at two positions close to the pistons, is measured with linear potentiometers with an accuracy of <1 μm. This information is required to determine the area of the side of the model, which is used to calculate the flow stress.

Thermal imaging

In addition to the bulk rheology, we plan to map the detailed rheology of the models. The material distribution and the temperature field are essential for this purpose. The former is determined by monitoring passive material markers with an optical camera; the latter is recorded using a thermal infrared camera.

Because the confining glass side walls have thermal diffusivities similar to the analogue materials, the temperature distribution can be mapped through the glass. The thermal energy (between wavelengths of 8 and 12 μm) radiated from the glass is recorded by the camera with a resolution of ~36 temperature pixels/cm^2. Assuming black body radiation, these energy values can be converted to apparent surface temperature.

In our model, the glass wall is far from being a black body; glass is rather reflective in the infrared part of the spectrum. To calibrate the temperature scale, we used a probe to measure the temperature at various positions in the middle of the model, in a section parallel to the glass walls (Fig. 2A). The measured temperatures were then correlated with the values measured by the camera to produce the colorscale for the infrared images given in Figure 2B.

SCALING

Analogue experiments must be designed in a way that they are similar to nature in the relevant aspects. To model nature, the equations that represent these aspects must be accurately scaled, a concept described by Hubbert (1937). Here we present a brief analysis of the significant equations. A more detailed analysis was given by Cobbold and Jackson (1992).

Time

In our experiments we take advantage of the differences in rheology induced by the thermal gradient within the material. The equation governing heat transfer in thermally isotropic materials, without internal heat production, is

$$\frac{dT}{dt} = \frac{\partial\left(a\dfrac{\partial T}{\partial x_i}\right)}{\partial x_i}, \quad (6)$$

where T is the temperature field, x_i are the three dimensions of space, and a denotes the thermal diffusivity.

During deformation, thermal and mechanical velocities must be treated equally. Thus, we have to ensure that the time needed by material particles or heat to move over a certain distance is scaled by the same factor. For the scaling factors of length l, time t, and thermal diffusivity a, we therefore obtain

$$S_t = \frac{S_l^2}{S_a}, \quad (7)$$

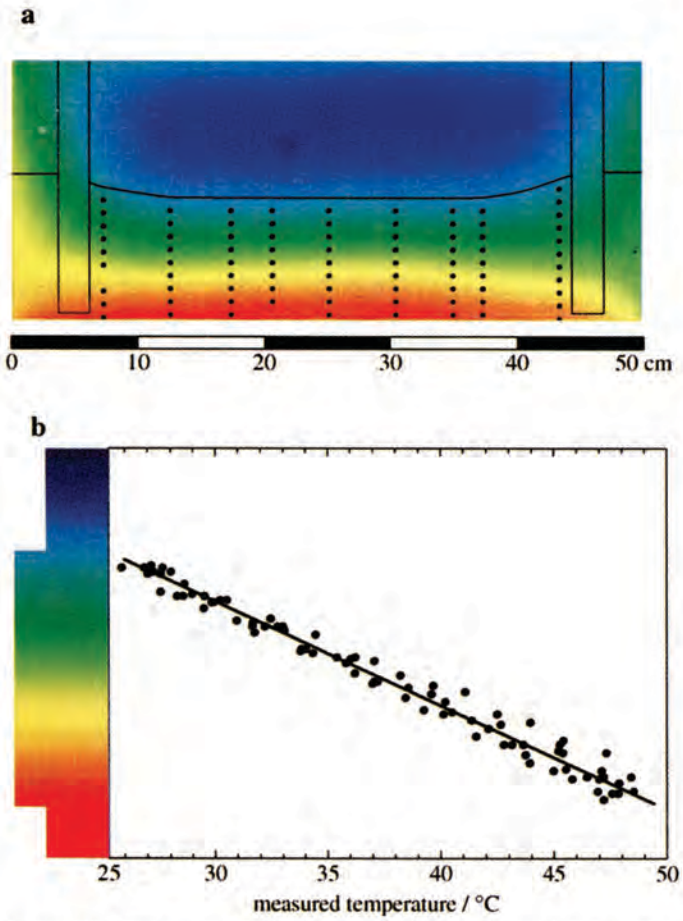

Figure 2. Temperature calibration. A: Scale of infrared camera (obtained from outside surface of side wall) calibrated by measuring actual temperature within model, using temperature probe at positions shown. Material surface and pistons are indicated. B: Temperatures measured at positions given in A correlated with energy values obtained from camera (color). Correlation is linear. Clustering of values is due to homogeneous temperature gradient.

where the scaling factors S_X of a property X represent the ratio of laboratory values to natural values. Equation 7 couples the length and time scales to the material-dependent scale of thermal diffusivity.

Stress

In the model, as in nature, gravity (g) acts on a material unit with a density ρ and a thickness h, resulting in gravitational stresses σ_{grav}. Gravitational stresses need to have the same scaling factor as viscous stresses σ_{visc}, where the latter result from deforming a material with a viscosity η at a strain rate $\dot{\varepsilon}$. Because

$$\sigma_{visc} = \eta\dot{\varepsilon} \tag{8}$$

and

$$\sigma_{grav} = \rho g h, \tag{9}$$

the model is only scaled to gravity when

$$S_\eta = S_\rho S_g S_l S_t. \tag{10}$$

Temperature

To check the scaling factor for the absolute temperature T we have to consider the Arrhenius equation

$$\eta(T) = \eta_0 e^{H/(RT)} \tag{11}$$

(after Pahl et al., 1991), where R is the universal gas constant and H is the activation energy. This equation does not influence the scale factor for viscosity, but it does require the exponent to be dimensionless. Because $S_R = 1$,

$$S_H = S_T. \tag{12}$$

FIRST EXPERIMENTS

Setup

The aim of the first experimental runs was to test the possibility of modeling the deformation of isotherms in thrust tectonics. Appropriate analogue materials for which viscosity depends on strain rate and temperature are, e.g., colophony (Cobbold and Jackson, 1992) or paraffin wax (e.g., Mancktelow, 1988; Rossetti et al., 1999). We decided to use paraffin wax because it is easier to work and layers with different rheologies can be constructed. The experiment presented here consisted of two 5-cm-thick layers of paraffin wax with different melting points. The melting points, T_m, for the lower and upper layers were 53 ± 1 and 43 ± 1 °C, respectively. Both paraffin waxes were supplied by MERCK, Darmstadt.

To produce overthrusting, the model was cut in the middle at an angle of 30°. To prevent the cut from annealing during the preheating phase, it was lubricated with Vaseline. Without introducing such an inhomogeneity, the model would deform homogeneously, or the deformation would concentrate at the pistons.

The model was set up in such a way that the underthrust slab would start melting after moving about halfway down the thrust. To keep the experiment as simple as possible, both layers were kept above the phase-transition temperature for the corresponding paraffin wax (e.g., Mancktelow, 1988; Rossetti et al., 1999). This led to a base temperature of 51 °C, a surface temperature of 25 °C, and the wax layer interface temperature of 38 °C. Neglecting strain rate and assuming that the rheology is only dependant on the homologous temperature T/T_m, this corresponds to the rheology profile given in Figure 3.

Scaling

The thermal diffusivity of natural rocks is about 10^{-6} m^2 s^{-1} (e.g., Turcotte and Schubert, 1982; Fowler, 1990), whereas that

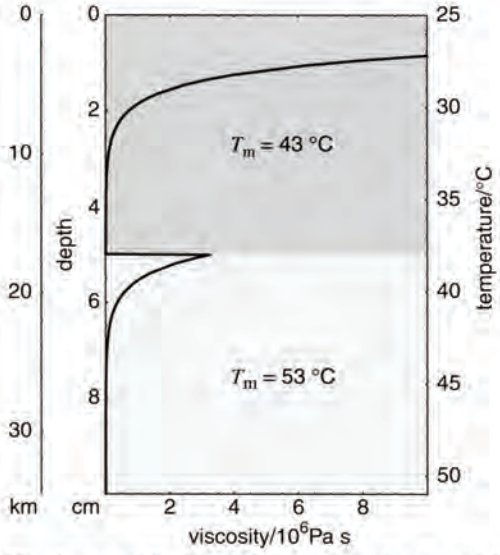

Figure 3. Rheology profile of initial state of two-layer model. Viscosities of lower layer are obtained using data from Rossetti et al. (1999), who described similar wax. For upper layer it was assumed that viscosities only depend on homologous temperature T/T_m. Viscosity at surface is 6.8×10^7 Pa s. Laboratory and natural depth scales are given.

of paraffin wax is about 8×10^{-8} m^{2}s^{-1} (Rossetti et al., 1999). This results in a scaling factor of 8×10^{-2}. Orogenic processes have strain rates on the order of 10^{-14} s^{-1} (Pfiffner and Ramsay, 1982). For the experiment, we decided to use the fastest possible strain rate of 9.5×10^{-5} s^{-1}. From the resulting scale factor for time of 1.05×10^{-10} and using equation 7, the scale factor for length is found to be 2.9×10^{-6}. Therefore, the initial model length of 50 cm corresponds to a length in nature of about 170 km.

The activation energy for paraffin waxes is ~1000 kJ/mol (Rossetti et al., 1999). For crustal rocks such as quartzites and granites it is around 150–200 kJ/mol (Carter and Tsenn, 1987). This results in a scale factor for the activation energy of 5–6. The temperature at the model base is 51 °C. The natural temperature at a depth of 34 km would be ~700 °C, assuming a geothermal gradient of 20 °C/km (e.g., Decker et al., 1988). These values lead to a scale factor of 0.3 for the temperature. If equation 12 were fulfilled, the model temperatures would have to be higher than the temperatures in nature. Because this is not possible, viscosity in the model depends too strongly on temperature. Therefore, for correct scaling, the rheology profile shown in Figure 3 should be flatter. Following an argument of Cobbold and Jackson (1992, p. 257), only the first two or three orders of magnitude of the overall strength variation are likely to have significant mechanical consequences. Therefore, true thermal scaling is probably unnecessarily rigorous.

Applying equation 10 to the scale factors for time and length and to the densities given in Table 1, we obtain a scaling factor for viscosities of 10^{-16} for the case of $S_g = 1$. According to Figure 3, the viscosity at the wax interface should be around

TABLE 1. EXPERIMENTAL PARAMETERS

Quantity		Nature	Laboratory	Scale
Thermal diffusivity	a	10^{-6} m^{2}s^{-1}	8×10^{-8} m^{2}s^{-1}	8×10^{-2}
Strain rate	$\dot{\varepsilon}$	10^{-14} s^{-1}	9.5×10^{-5}/s	9.5×10^{9}
Length	l	170 km	50 cm	2.9×10^{-6}
Time	t	1.16 Ma	3800 s	1.05×10^{-10}
Density	ρ	2700 kg m^{-3}	900 kg m^{-3}	0.33
Viscosity	η	10^{22} Pa s	3×10^{6} Pa s	10^{-16}
Activation energy	H	200 kJ/mol	1000 kJ/mol	5
Temperature	T	740 °C	51 °C	
		980 K	324 K	0.3

3×10^6 Pa s. Published flow parameters of rocks yield a broad range of viscosities. On the basis of parameters from Carter and Tsenn (1987) and assuming a temperature of 370 °C, crustal rocks at a depth of 17 km have viscosities ranging from 2×10^{20} Pa s to 4×10^{21} Pa s. Values taken from Kirby and Kronenberg (1987) give viscosities between 2×10^{22} Pa s and 10^{24} Pa s. This leads to actual factors for viscosity of 2×10^{-14} to 3×10^{-18}, which includes the required value of 1×10^{-16}. At greater depths these relations do not hold because of the reasons given herein.

Results

Analysis of the data recorded during the deformation of the model shows that the strain rate was constant. The mean strain rate over the entire experiment was 9.5×10^{-5} s^{-1}, with a standard deviation of 0.8×10^{-5} s^{-1} (Fig. 4). The deviations are purely statistical and depend only on the sampling rate. No trend can be observed. We can therefore assume constant rheology, at least locally, during the experiment.

The recorded force applied to the model (Fig. 5) increased to a peak value of almost 60 N, followed by a decrease to around 40 N, caused by strain softening.

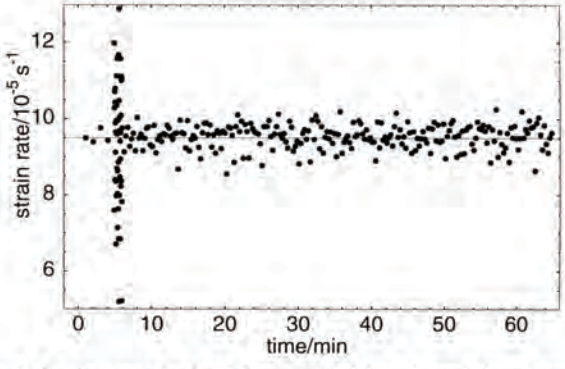

Figure 4. Strain rate obtained from model length and time intervals. Note that short intervals at beginning (every second, as opposed to every minute later on) lead to broader scatter of values. Thin line indicates required value.

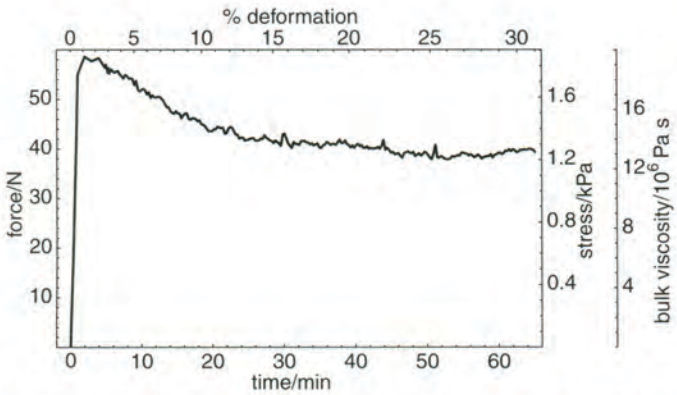

Figure 5. Force applied to model during deformation versus time and deformation. After initial rise, strain softening occurs. Stress and bulk viscosity are proportional to force due to constant strain rate and surface. Total area in x-y plane did not change due to isostatic equilibration.

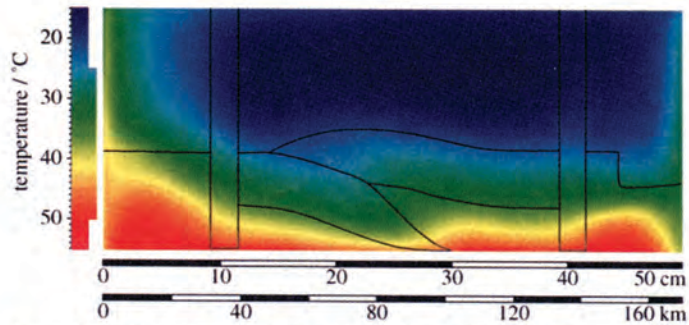

Figure 6. Infrared image of final state of described experiment. Material boundaries and pistons are shown.

Figure 6 shows the infrared image of the final stage of the experiment. The infrared image is overlain by outlines of the pistons and of the analogue-material boundaries obtained from an optical photograph (Fig. 7). It can be seen that the overthrusting material transports heat upward, while the underthrusting slab causes a downward bend in the isotherms. Due to the strong deflection of the isotherms, the subducting slab in the thickened crust did not cross the melting isotherm. For the given parameters, the advection of heat due to movement of the material is faster than equilibration by conduction.

CONCLUSIONS AND OUTLOOK

We have not attempted to interpret these results in a geological context. The primary aim of these initial simple experiments was to test the feasibility of thermotectonic modeling under controllable conditions.

Experiments such as the one presented here offer an unparalleled possibility to calibrate numerical models involving heat flow (e.g., Jamieson et al., 1996). These models could be calibrated against our results and then readjusted accordingly. Numerical models are limited by the exactness of the equations involved and their thermomechanical coupling. However, they overcome the shortcomings of our apparatus, especially the inability to obtain the exact scaling of all aspects of the experiment with the analogue materials used. Both techniques suffer from poorly defined flow laws of rocks under natural conditions (Handy, 2000).

The apparatus described here can perform thermomechanical experiments because a steady-state thermal gradient is induced by controlling heat flow into the bottom and out of the top of the model. This yields precise and controllable viscosity gradients within the analogue material. The detailed tempera-

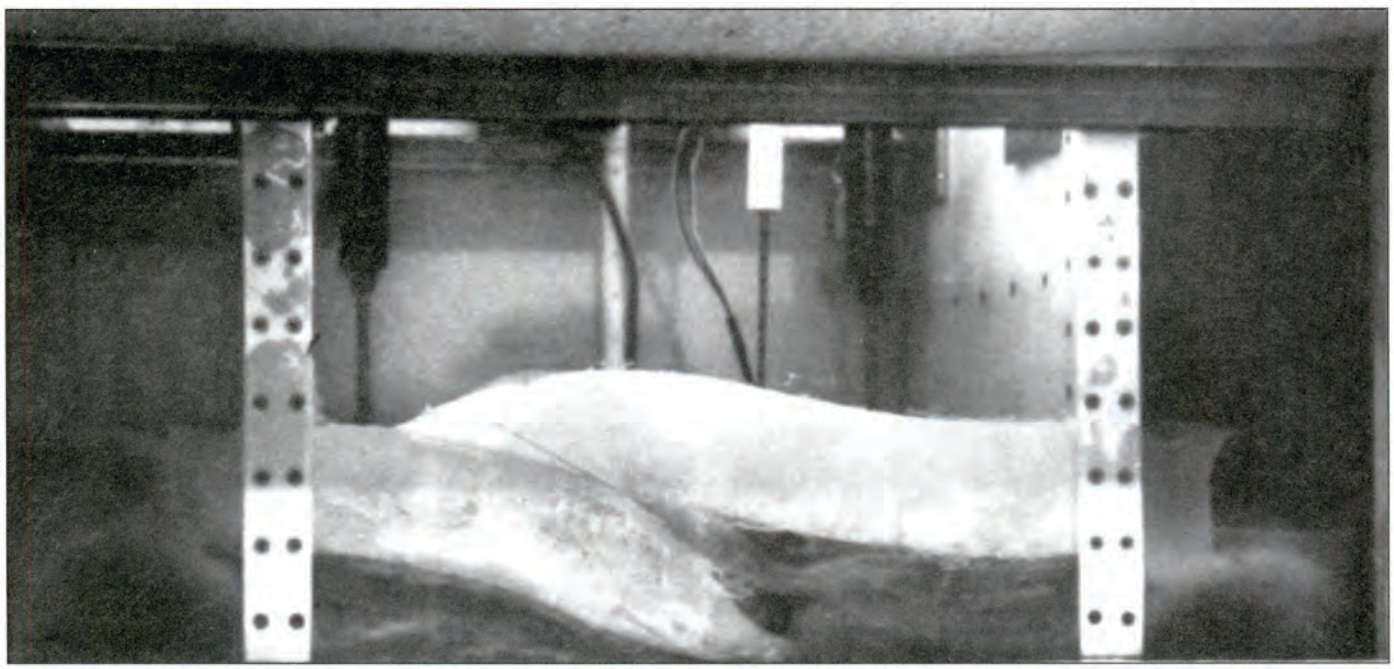

Figure 7. Photograph of final stage of described experiment. Two originally horizontal layers of paraffin wax were shortened by ~30%. Width of photograph is 50 cm.

ture distribution and hence the rheology can be obtained using a thermal infrared camera. From the temperature field and the material distribution, the viscosity can be calculated for each pixel, allowing an estimation of the time-dependent viscosity distribution. In future experiments we will introduce a brittle layer with Mohr-Coulomb behavior to represent the upper crust. Plastic powder (Jet-Plast) has an angle of internal friction of 35° and its bulk density of 0.75 kg/l allows gravity to be scaled correctly for the entire three-layer model. Experiments with constant convergence rates will be used to analyze geologically relevant scenarios. The relationship between the structures produced and the convergence rate will also be examined. The results obtained will further improve our understanding of the interaction between deformation and temperature distribution.

ACKNOWLEDGMENTS

We greatly appreciate the assistance we received from many colleagues and students. In particular, we thank Sigrid Dachnowsky, Alfred Immler, and Neil Mancktelow. We are indebted to Friedemann Burr for lease of the infrared camera. Image processing was done by Dennis Gross. The manuscript benefited from the thoughtful reviews of Phillipe Davy, Benoît Ildefonse, and Neil Mancktelow. The English was greatly improved by David Tanner. Financial support of the project by the Deutsche Forschungsgemeinschaft (Project BE 1041/11) is gratefully acknowledged.

REFERENCES CITED

Brune, J.N., and Ellis, M.A., 1997, Structural features in a brittle-ductile wax model of continental extension: Nature, v. 387, p. 67–70.

Carter, N.L., and Tsenn, M.C., 1987, Flow properties of continental lithosphere: Tectonophysics, v. 136, p. 27–63.

Chemenda, A.I., Mattauer, M., Malavieille, J., and Bokun, A.N., 1995, A mechanism for syn-collisional rock exhumation and associated normal faulting: Results from physical modeling: Earth and Planetary Science Letters, v. 132, p. 225–232.

Cobbold, P.R., and Jackson, M.P.A., 1992, Gum rosin (colophony): A suitable material for thermomechanical modeling of the lithosphere: Tectonophysics, v. 210, p. 255–271.

Davy, P., and Cobbold, P.R., 1991, Experiments on shortening of a 4-layer model of the continental lithosphere: Tectonophysics, v. 188, p. 1–25.

Decker, E.R., Heasler, H.P., Buelow, K.L., Baker, K.H., and Hallin, J.S., 1988, Significance of past and recent heat-flow and radioactivity studies in the southern Rocky Mountains region: Geological Society of America Bulletin, v. 100, p. 1851–1885.

Fowler, C.M.R., 1990, The solid Earth: Cambridge, Cambridge University Press, 472 p.

Grujic, D., Casey, M., Davidson, C., Hollister, L.S., Kündig, R., Pavlis, T., and Schmid, S., 1996, Ductile extrusion of the Higher Himalayan Crystalline in Bhutan: Evidence from quartz microfabrics: Tectonophysics, v. 260, p. 21–43.

Handy, M.R., ed., 2000, Rheology and geodynamic modelling: The next step forward: International Journal of Earth Sciences (Geologische Rundschau), (in press).

Hubbert, M.K., 1937, Theory of scale models as applied to the study of geologic structures: Geological Society of America Bulletin, v. 48, p. 1459–1519.

Jamal, R., and Pichlik, H., 1997, LabVIEW: Programmiersprache der vierten Generation: Munich, Prentice-Hall, 532 p.

Jamieson, R.A., Beaumont, C., Hamilton, J., and Fullsack, P., 1996, Tectonic assembly of inverted metamorphic sequences: Geology, v. 24, p. 839–842.

Kirby, S.H., and Kronenberg, A.K., 1987, Rheology of the lithosphere: Selected topics: Reviews of Geophysics, v. 25, p. 1219–1244.

Mancktelow, N.S., 1988, The rheology of paraffin wax and its usefulness as an analogue for rocks: Uppsala University Geological Institutions Bulletin, v. 14, p. 181–193.

Mancktelow, N.S., 1995, Nonlithostatic pressure during sediment subduction and the development and exhumation of high pressure metamorphic rocks: Journal of Geophysical Research, v. 100, p. 571–583.

Nataf, H.C., and Richter, F.M., 1982, Convection experiments in fluids with highly temperature-dependent viscosity and the thermal evolution of the planets: Physics of the Earth and Planetary Interiors, v. 29, p. 320–329.

Oldenburg, D.W., and Brune, J.N., 1972, Ridge transform fault spreading pattern in freezing wax: Science, v. 178, p. 301–304.

Oldenburg, D.W., and Brune, J., 1975, An explanation for the orthogonality of ocean ridges and transform faults: Journal of Geophysical Research, v. 80, p. 2575–2585.

Pahl, M.H., Geißle, W., and Laun, H.-M., 1991, Praktische Rheologie der Kunststoffe und Elastomere: Düsseldorf, Germany, VDI-Verlag, 428 p.

Pfiffner, O.A., and Ramsay, J.G., 1982, Constraints on geological strain rates: Arguments from finite strain states of naturally deformed rocks: Journal of Geophysical Research, v. 87, p. 311–321.

Rossetti, F., Ranalli, G., and Faccenna, C., 1999, Rheological properties of paraffin as an analogue material for viscous crustal deformation: Journal of Structural Geology, v. 21, p. 413–417.

Shemenda, A.I., and Grocholsky, A.L., 1994, Physical modeling of slow seafloor spreading: Journal of Geophysical Research, v. 99, p. 9137–9153.

Turcotte, D.L., and Schubert, G., 1982, Geodynamics. Application of continuum physics to geological problems: New York, John Wiley & Sons, 450 p.

MANUSCRIPT ACCEPTED BY THE SOCIETY APRIL 12, 2000

Printed in the U.S.A.